

1 **Influence of gap size, screw configuration and nail materials in the stability of**
2 **anterograde reamed intramedullary nail in femoral transverse fractures**

3
4 S. Gabarre¹, J. Albareda^{2,3,4§}, L.Gracia^{1,5}, S. Puértolas^{1,5}, E. Ibarz^{1,5}, A. Herrera^{3,4}

5
6
7
8
9
10
11
12
13
14
15
16
17
18
19
20
21
22
23
24
25
26
27
28
29
30
31
32
33
34
35
36
37
38
39
40
41
42
43
44
45
46
47
48
49
50
51
52
53
54
55
56
57
58
59
60
61
62
63
64
65
66
67
68
69
70
71
72
73
74
75
76
77
78
79
80
81
82
83
84
85
86
87
88
89
90
91
92
93
94
95
96
97
98
99
100
101
102
103
104
105
106
107
108
109
110
111
112
113
114
115
116
117
118
119
120
121
122
123
124
125
126
127
128
129
130
131
132
133
134
135
136
137
138
139
140
141
142
143
144
145
146
147
148
149
150
151
152
153
154
155
156
157
158
159
160
161
162
163
164
165
166
167
168
169
170
171
172
173
174
175
176
177
178
179
180
181
182
183
184
185
186
187
188
189
190
191
192
193
194
195
196
197
198
199
200
201
202
203
204
205
206
207
208
209
210
211
212
213
214
215
216
217
218
219
220
221
222
223
224
225
226
227
228
229
230
231
232
233
234
235
236
237
238
239
240
241
242
243
244
245
246
247
248
249
250
251
252
253
254
255
256
257
258
259
260
261
262
263
264
265
266
267
268
269
270
271
272
273
274
275
276
277
278
279
280
281
282
283
284
285
286
287
288
289
290
291
292
293
294
295
296
297
298
299
300
301
302
303
304
305
306
307
308
309
310
311
312
313
314
315
316
317
318
319
320
321
322
323
324
325
326
327
328
329
330
331
332
333
334
335
336
337
338
339
340
341
342
343
344
345
346
347
348
349
350
351
352
353
354
355
356
357
358
359
360
361
362
363
364
365
366
367
368
369
370
371
372
373
374
375
376
377
378
379
380
381
382
383
384
385
386
387
388
389
390
391
392
393
394
395
396
397
398
399
400
401
402
403
404
405
406
407
408
409
410
411
412
413
414
415
416
417
418
419
420
421
422
423
424
425
426
427
428
429
430
431
432
433
434
435
436
437
438
439
440
441
442
443
444
445
446
447
448
449
450
451
452
453
454
455
456
457
458
459
460
461
462
463
464
465
466
467
468
469
470
471
472
473
474
475
476
477
478
479
480
481
482
483
484
485
486
487
488
489
490
491
492
493
494
495
496
497
498
499
500
501
502
503
504
505
506
507
508
509
510
511
512
513
514
515
516
517
518
519
520
521
522
523
524
525
526
527
528
529
530
531
532
533
534
535
536
537
538
539
540
541
542
543
544
545
546
547
548
549
550
551
552
553
554
555
556
557
558
559
560
561
562
563
564
565
566
567
568
569
570
571
572
573
574
575
576
577
578
579
580
581
582
583
584
585
586
587
588
589
590
591
592
593
594
595
596
597
598
599
600
601
602
603
604
605
606
607
608
609
610
611
612
613
614
615
616
617
618
619
620
621
622
623
624
625
626
627
628
629
630
631
632
633
634
635
636
637
638
639
640
641
642
643
644
645
646
647
648
649
650
651
652
653
654
655
656
657
658
659
660
661
662
663
664
665
666
667
668
669
670
671
672
673
674
675
676
677
678
679
680
681
682
683
684
685
686
687
688
689
690
691
692
693
694
695
696
697
698
699
700
701
702
703
704
705
706
707
708
709
710
711
712
713
714
715
716
717
718
719
720
721
722
723
724
725
726
727
728
729
730
731
732
733
734
735
736
737
738
739
740
741
742
743
744
745
746
747
748
749
750
751
752
753
754
755
756
757
758
759
760
761
762
763
764
765
766
767
768
769
770
771
772
773
774
775
776
777
778
779
780
781
782
783
784
785
786
787
788
789
790
791
792
793
794
795
796
797
798
799
800
801
802
803
804
805
806
807
808
809
810
811
812
813
814
815
816
817
818
819
820
821
822
823
824
825
826
827
828
829
830
831
832
833
834
835
836
837
838
839
840
841
842
843
844
845
846
847
848
849
850
851
852
853
854
855
856
857
858
859
860
861
862
863
864
865
866
867
868
869
870
871
872
873
874
875
876
877
878
879
880
881
882
883
884
885
886
887
888
889
890
891
892
893
894
895
896
897
898
899
900
901
902
903
904
905
906
907
908
909
910
911
912
913
914
915
916
917
918
919
920
921
922
923
924
925
926
927
928
929
930
931
932
933
934
935
936
937
938
939
940
941
942
943
944
945
946
947
948
949
950
951
952
953
954
955
956
957
958
959
960
961
962
963
964
965
966
967
968
969
970
971
972
973
974
975
976
977
978
979
980
981
982
983
984
985
986
987
988
989
990
991
992
993
994
995
996
997
998
999
1000

¹ Department of Mechanical Engineering, University of Zaragoza. Zaragoza, Spain

² Department of Orthopaedic Surgery and Traumatology, Lozano Blesa University Hospital. Zaragoza, Spain

³ Aragón Health Research Institute. Zaragoza, Spain

⁴ Department of Surgery, University of Zaragoza. Zaragoza, Spain

⁵ Aragón Institute for Engineering Research. Zaragoza, Spain

[§] Corresponding author:

E-mail: albaredajorge@gmail.com

Address: Medicine School
University of Zaragoza
Domingo Miral, s/n
50009 – Zaragoza (SPAIN)

Email addresses:

SG : sergioga@unizar.es Sergio Gabarre

LG: lugravi@unizar.es Luis Gracia

SP: spb@unizar.es Sergio Puértolas

EI: eibarz@unizar.es Elena Ibarz

AH: antonio.herrera@unizar.es Antonio Herrera

10 **ABSTRACT**

11

12 Femoral shaft fractures are among the most serious of the skeleton and present high
13 morbidity and mortality in addition to important complications and consequences. So,
14 the most appropriate treatment depending on the type of fracture and location level
15 should be chosen.

16

17 A finite element model of the femur has been developed, analysing various types of
18 fractures in the subtrochanteric and diaphyseal supracondylar area, with several gap
19 sizes, stabilizing with a single combination of screws for the intramedullary nail. The
20 mechanical strength of the nail against bending and compression efforts was studied
21 comparing two materials for the nail: stainless-steel and titanium alloy

22

23 Beside the FE simulations, a clinical follow-up was realized, considering a sample of 55
24 patients, 24 males and 31 females, with mean age of 52.5 years. Localizations of
25 fractures were 22 in the right femur and 33 in the left femur, respectively.

26

27 A good agreement between clinical results and the simulated fractures in terms of gap
28 size was found. Non-comminuted fractures have a mean consolidation time of 4.1
29 months, which coincides with the appropriate mobility at fracture site obtained in the
30 FE simulations, whereas comminuted fractures have a higher mean consolidation period
31 estimated in 7.1 months, corresponding to the excessive mobility at fracture site
32 obtained by means of FE simulations.

33

34 The obtained results between both nail materials (stainless steel and titanium alloy)
35 show a higher mobility when using a titanium nails, which produce a higher rate of
36 strains at the fracture site, amplitude of micromotions and bigger global movements
37 compared to stainless steel nails. Steel nails provide stiffer osteosyntheses than the
38 titanium nails.

39

40 In conclusion, the anterograde locked nail is particularly useful in the treatment of a
41 wide range of supracondylar fractures with proximal extension into the femoral
42 diaphysis.

43 **Key terms:** Intramedullary nail, Anterograde reamed nail, Femoral fracture, Gap
44 analysis, Osteosynthesis, Finite element analysis.

45

46 **INTRODUCTION**

47

48 Femoral shaft fractures are among the most serious of the skeleton, characterized by
49 high morbidity and mortality in addition to presenting important complications and
50 consequences [1, 2]. Therefore, they must be treated being conscious of its complexity
51 looking for the most appropriate treatment depending on the type of fracture and
52 location level.

53

54 In the 1940s G Küntscher [3] introduced the intramedullary nailing (IM). In the 60's,
55 tibial and femoral compression plates slowed the expansion of nailing. But, from the
56 70's, nailing has gradually become the first choice in the treatment of diaphyseal
57 fractures of long bones. Since the 80's, many changes have been performed in order to
58 improve results such as: design of the nails, morphology, materials, locking system and
59 placement technique, allowing the locked intramedullary nails to become the standard
60 of care for most femoral fractures.

61

62 Their indication has been extended to almost all femoral proximal and distal fractures:
63 running from the lesser trochanter to the supracondylar area zones 2 (subtrochanteric)
64 and 5 (supracondylar) of Wiss [4, 5]. It can be said that at present locked intramedullary
65 nailing is the most suitable technique to treat femoral fractures. The advantages of IM
66 nailing are: is a closed technique, preserves the hematoma in the focus of fracture,
67 permits an easier extraction [5], exhibits a high rate of consolidation (98%) and a low
68 percentage of infection (1%).

69

70 Although several improvements in IM nails have been developed, some complications
71 remain as fatigue failure, non-union, bone-fracture and screw loosening. Reducing the
72 stiffness of nail material can contribute to diminish stress-shielding and thus accelerate
73 healing process [6]. When too flexible materials are used, some problems associated
74 with load transfer such as loosening, malunion or poor-union appear [7, 8].

75 Controversial results about rigidity of the implant have been reported leaving optimum
76 fixation stiffness as a pending issue [7].

77

78 The indications for anterograde intramedullary nailing are essentially extra-articular
79 fractures, inclusive in the rare cases of bi- or trifocal fractures of the distal femur, where
80 nailing is often the only therapy [9]. The biggest controversy about their indication lies
81 on the fractures located on the distal third of the femur, which although infrequent
82 present major difficulties for their treatment. The estimated frequency is 0.4% of all
83 fractures and 3% of femoral fractures [10]. Different treatments have been proposed for
84 this type of fracture: blade plate, dynamic compression plate, locking compression
85 plate, anterograde nailing or retrograde nailing [9]. However, the anterograde nailing
86 with the new implants offer multiple distal screw position options that allow articular
87 reconstruction and sturdy fixation even in intra-articular fractures [11].

88

89 Despite the multiple designs, techniques and materials, the static locking intramedullary
90 nail remains the reference treatment of femur fractures located between Zones 2 and 5
91 of Wiss [4, 12, 13]. The ultimate success depends on the treatment according to the
92 characteristics of the fracture, the habits of the patient, associated lesions and the
93 surgeon's experience with the used technique [9, 14]. The great diversity of types of
94 diaphyseal fracture, according to their anatomical location and degree of comminution,
95 makes it difficult on multiple occasions the choice of nailing and locking to ensure
96 stability and to achieve fracture consolidation. Therefore multiple experimental works
97 to study the biomechanical behavior of different type of nailing and locking them have
98 been done.

99

100 In vivo animal experimentation on biomechanical behaviour of intramedullary femoral
101 nails has a difficult extrapolation to humans due to anatomical differences and load
102 conditions. Similarly, in vitro studies experiments on cadaveric bone or plastic bone
103 models [15], can hardly be applied to humans, due to the differences between in vivo
104 and in vitro behaviour. Those difficulties have led to the development of simulation
105 models using the finite element method (FE). Analysis of osteosynthesis by means of a
106 FE models enables the assessment of all critical parameters, such as maximum
107 permissible load on the nail, local movements at the fracture site and stress
108 concentrations around the locking screws.

109

110 Few studies have been published on experimental or computational models based on FE
111 method applied to intramedullary nailing investigation of femoral shaft fractures. So,
112 Regarding femoral nailing, Wang [16] analyzes the behaviour of short nails in the
113 management of proximal femoral fractures, by comparing two fixation screws and
114 studies the stiffness of the distal end in a posterior work [17]. Reference [18] studies a
115 gamma nail design made in two different materials: titanium and stainless steel. Cheung
116 performed a study on long nails [19] comparing FE simulation with experimental tests
117 results, analyzing the differences in the relative stiffness between healthy and nailed
118 femur. More recently, reference [20] analyzes the mechanical behaviour of a single
119 screw with the use of two distal locking screws in a gamma locking nail. Chen studied
120 distal femoral fractures managed with short nails by analyzing the differences in
121 stiffness between the healthy and the nailed femur [21] . Fracture stability for flexible
122 nails used in pediatrics was studied, modifying nail stiffness, in [22]. In [23] the
123 influence of muscle forces on failure of distal nail holes and locking screws is studied.
124 In [24] a combination of experimental and numerical methods is used to evaluate the
125 stress distribution in an anterograde intramedullary nail. In [25, 26] a comparison
126 between nails and locking plates in a metaphyseal wedge fracture in synthetic
127 osteoporotic bone is executed. Static versus dynamic fixation techniques are compared
128 in [27]. Finally, in [13] a comparison of strain magnitude and distribution resulting from
129 two different entry points for anterograde nailing is performed.

130

131 **WORK OBJECTIVES**

132

133 The present study pretends to evaluate the stability of an IM Stryker femoral nail S2
134 (Stryker, Mahwah, NJ, USA). A FE model of the femur has been developed, analysing
135 various types of fractures in the subtrochanteric and diaphyseal supracondylar area,
136 stabilizing with one combination of screws, studying the mechanical strength of the nail
137 against bending and compression efforts, to determine its maximum resistant capacity.
138 Two materials were studied for the metallic nail: 316 LVM stainless-steel and Ti-6Al-
139 4V alloy. A comparative analysis of the different types of osteosynthesis at different
140 fractures was done, in order to verify the optimal solution in each case of those
141 analyzed.

142

143 **2.-MATERIALS & METHODS**

144

145 **2.1.-Modelling of the femur and implants**

146

147 A three dimensional (3D) finite element model of the femur from 55 year old male
148 donor was developed. Outer Geometry of the femur was obtained by means of 3D
149 scanner Roland3D Roland® PICZA (Irvine, California) scanner, whereas a set of
150 computed tomography (CT) of the donor's femur were treated using Mimics® Software
151 (Materialise, Leuven). Once the inner interface between cortical and trabecular bone
152 was determined, by means of an in-house algorithm material properties were assigned to
153 the FE model in I-Deas [28], using the same workflow of a previous study [29].

154

155 The studied femoral nail Stryker S2™ (Stryker, Mahwah, NJ, USA) was 380 mm long,
156 with a wall thickness of 2 mm and an outer diameter of 13 mm. This reamed
157 antegrade nail uses locking screws of 5 mm of outer diameter, which were modelled
158 as cylinders of the same diameter.

159

160 **2.2.-Meshing and material properties**

161

162 Nail surgery was reproduced in I-Deas in a virtual way, inserting the nail into the femur
163 with the corresponding screws. Afterwards the assembly of the computer aided design
164 (CAD) model was performed under surgeon supervision. Bone, nail and screws were
165 meshed with linear tetrahedra. They were assumed for the bone linear elastic isotropic
166 properties ($E_{\text{Cortical}}=20000$ MPa, $\nu=0.3$; $E_{\text{Trabecular}}=959$ MPa, $\nu=0.3$ [30], as reference),
167 with variable values related with the processed CT images. The metallic nail was made
168 of 316 LVM steel ($E=192.36$ GPa, $\nu=0.3$) or Ti-6L-4V ($E=113.76$ GPa, $\nu=0.34$) and
169 metallic screws of 316 LVM steel, both assumed to be linear elastic isotropic.

170

171 A sensitivity analysis was performed to determine the minimal size mesh required for
172 an accurate simulation. For this purpose, a mesh refinement was performed in order to
173 achieve a convergence towards a minimum of the potential energy, both for the whole
174 model and for each of its components, with a tolerance of 1% between consecutive
175 meshes.

176

177 2.3.- Configurations used and contact modelling

178

179 All the considered fractures were modelled as transverse by means of an irregular
180 surface developed to represent a closer geometry to the actual fracture. The effect of gap
181 size remains unclear in the literature. So, the majority of the reviewed in vivo studies
182 are referred to a gap size ranging from 0.6 to 6 mm [31, 32] whereas in FE simulation
183 articles it ranged from 0.7 to 10 mm. [33, 34].

184

185 Thus, using this irregular fracture pattern, three different fracture gaps have been
186 studied: 0.5 mm (considered as a non-comminuted fracture), 3 mm (as the most
187 referenced value found in literature, representing a mid-value) and 20 mm as an
188 example of comminuted fracture (Fig. 1). In addition to this, three localizations of the
189 fracture were studied: proximal, medial and distal for each gap size. Only one
190 combination of screws was studied: one oblique placed proximally and two transverse
191 at the distal part. Table 1 summarizes the list of FE models simulated for the three gap
192 sizes.

193

194 The study was focused on the immediately post-operative stage. Thus, the interaction at
195 the fracture site does not take into account any biological healing process. Contact
196 interaction was assumed between the outer surface of the nail and the inner cortex of the
197 medullary canal of the femur (Fig. 2). Interaction between screws and cortical bone was
198 considered to be bonded, whereas contact between screws a femoral nail was simulated.
199 The selected friction values of bone/nail and nail/screws were 0.1 and 0.15,
200 respectively, in accordance with literature [34-36]. Other similar studies modelled
201 bone/nail interaction as frictionless, though [24, 37].

202

203 2.4.- Loads and boundary conditions

204

205 This study considered fully constrained conditions at the condyles and a load case
206 associated with an accidental support of the leg at early post-operative (PO) stage (Fig.
207 3). This load was quantified to be about 25% the maximum gait load. According to
208 Orthoload's database, the hip reaction force and abductor force (as the prime muscle
209 group), referred to the 45% of gait, correspond to the maximum and most representative

210 load [38]. Muscle attachments areas corresponding to abductor group muscle were
211 determined mimicking anatomy atlas.

212

213 2.5.- Clinical follow-up

214

215 Beside the FE simulations, a clinical follow-up was realized, considering a sample of 55
216 patients, 24 males and 31 females, with mean age of 52.5 years, all of them treated with
217 femoral nail Stryker S2TM. Localizations of fractures were 32 in the right femur and 33
218 in the left femur. The statistic corresponding to fracture localization and fracture grade
219 are included in Table 2. The comminute grade was measured according to the scale of
220 Winquist/Hansen [39].

221

222 **3.-RESULTS**

223

224 The FE simulations allow obtaining the mobility results for the different cases analyzed.
225 Figure 4 shows the deformed shape amplified (x25) and the vertical displacement maps
226 corresponding to fractures non-comminuted (gap size 0.5 mm) and comminuted (gap
227 size 20 mm).

228

229 In order to study relative micromotion at fracture site, pairs of homologue points at the
230 fracture site were identified, as nodes that were opposed as shown in Fig. 5.

231

232 When analysing results, Perren's method [28] gives a threshold strain value of 10%
233 beyond which fracture healing is expected to occur. This strain value is defined as the
234 relative motion in fracture gap divided by the original fracture gap. Tables 3a and 3b
235 shows the results associated to Perren method at the three fractures sites and gaps
236 studied for steel and titanium nails, respectively. This reference parameter strongly
237 depends on the fracture gap size. Thus, according to Table 3a healing condition is
238 fulfilled for all the fractures of 3 and 20 mm (comminuted) and the medial and distal
239 location for 0.5 mm gap size. On the other hand, Table 3b exhibit higher strains for
240 titanium nail compared to steel one, as none of the 0.5 mm gap fractures verify the
241 condition for callus formation. Thus this strain criterion should be considered with
242 caution. Conversely according to micromotion results, this parameter is not valid for

243 small fracture gaps as it gives strain values higher than 10% for proximal and medial
244 fracture location.

245

246 Tables 4a and 4b show the maximum amplitude of micromotion between homologue
247 points at the fracture site for steel and titanium nails, respectively. Table 4a shows that
248 the most rigid behaviour belongs to diaphyseal fracture (40.69-66.43 μm) followed by
249 medial one (51.96-73.39 μm) and proximal one (60.29-90.29 μm). Micromotion
250 amplitude follows the same growing tendency with the increase of the gap for all the
251 three fracture locations.

252

253 Table 4b show the same tendency for titanium at the three fracture locations observed
254 previously: micromotions at diaphyseal fracture ranges from 62.02 to 123.71 μm ,
255 followed by medial one (ranging from 75.88 to 139.80 μm) and finally proximal one
256 (varying from 93.07 to 140.83 μm). If the ratio of the amplitudes between both
257 materials is calculated, a pitchfork of 1.46 to 2.00 is obtained which is within the range
258 of the Young's modulus ratio for both materials (1.69).

259

260 Nevertheless, when evaluating the global stability reported in Table 5a and 5b, by
261 measuring the displacement at head of the nail (insertion point at trochanter) the trend is
262 reversed: proximal fracture is the most rigid, followed by medial fracture and distal
263 fracture. This result can be explained in terms of a basic concept of mechanics. Figure 6
264 shows a scheme of lever arms between proximal and diaphyseal fractures. Lever arm is
265 defined as the distance ("D" or "d") between the mid-plane of the fracture and the head of
266 the femur. For a proximal fracture, the lever arm is much shorter than for the distal
267 fracture. Consequently when applying the physiological loads at the head of the femur,
268 the IM nail blocks the global movement of the femoral head "sooner" for the proximal
269 fracture than for the diaphyseal one. According to gap size influence, there is a marked
270 increase in the interfragmentary movement as well as global stability when the gap
271 increases.

272

273 For steel nail, Table 5a values range from 1.33 mm (proximal fracture, 0.5 mm gap) to
274 2.01 mm (diaphyseal fracture, 20 mm. gap), whereas titanium nail yield to a higher rate
275 of global movement as Table 4b reports: 1.62 mm (proximal fracture, 0.5 mm gap) to

276 3.14 mm (diaphyseal fracture, 20 mm gap). Calculating the ratio of the global
277 movement between both materials a pitchfork of 1.22 to 1.56 is obtained.

278

279 With respect to the clinical follow-up, non-comminuted fractures have a mean
280 consolidation time of 4.1 months, whereas comminuted fractures (grade 4 Winquist and
281 Hansen) have a higher mean consolidation period estimated in 7.1 months. On the other
282 hand, intermediate comminution grades lead to longer mean consolidation periods than
283 non-comminuted fractures (4.9 months for grade 1 and 6.2 months for grade 2,
284 respectively. Grade 3 was not finally considered because only one case was reported).
285 So, the healing time increases inasmuch as the comminution grade is higher.

286

287 **4.-DISCUSSION**

288

289 Difficulties in vivo experimentation and the unreliability of in vitro models, has
290 conditioned the development of simulation models by FE that allow studying different
291 biological systems in both physiological and pathological conditions, and provide a
292 quick and easy testing in different conditions difficult to achieve experimentally.
293 However, they are still a very limited number of published papers which study the
294 behaviour of intramedullary nails in the femur. The models developed in the present
295 work allow the simulation of fracture in different locations, with different gap and
296 different alternatives of nailing (material and different locking system), and determine
297 whether the relative displacement at fracture site fall within acceptable limits, in order
298 to achieve the fracture healing. The stability of the fracture is essential for the
299 consolidation.

300

301 Fracture healing depends on general and local factors which may be modified by
302 extrinsic conditions, such as biomechanics of fracture fixation [40]. The excess of
303 movement at the fracture site adversely affects callus formation [32], resulting in lower
304 blood vessels content, a greater presence of fibrocartilage and a lower bone formation
305 [41, 42]. Therefore, relative displacements between bone fragments must be wide
306 enough to promote bone formation according to "Wolff's Law", without exceeding the
307 threshold value which prevents callus formation [32]. We simulated different types of
308 fractures located between Zones 2 and 5 of Wiss.

309

310 Although distal fracture (zone 5 of Wiss) is considered to be the most problematic area
311 in terms of fracture stability, anterograde intramedullary nailing is a suitable option to
312 provide stability at the fracture site [43]. It is important that the morphology of the
313 fracture allows the screw to be placed at least, at three centimetres of distance to the
314 fracture site [48].

315

316 Anterograde interlocked intramedullary nails have been used successfully in the
317 treatment of extra articular distal femoral fractures with 7 cm of intact distal femur or
318 when a 7-cm fragment could be reconstructed with accessory lag screws or distal
319 locking screws [44]. Large-diameter nails should be used to avoid fatigue fracture at the
320 screw holes. When necessary, the intramedullary nail can be shortened to decrease the
321 distance between the distal locking screw and the nail tip. The anterograde locked nail is
322 particularly useful in the treatment of supracondylar fractures with proximal extension
323 into the femoral diaphysis.

324

325 There is a good agreement between clinical results and the simulated fractures in terms
326 of gap size. Thus, non-comminuted fractures have a mean consolidation time of 4.1
327 months, which coincides with the appropriate mobility at fracture site obtained in the
328 FE simulations, whereas comminuted fractures (grade 4 Winquist and Hansen) have a
329 higher mean consolidation period estimated in 7.1 months, corresponding to the
330 excessive mobility at fracture site obtained by means of FE simulations.

331

332 On the other hand, the obtained values between both nail materials (Stainless steel and
333 titanium alloy) show a higher mobility when using titanium nails, which produce a
334 higher rate of strains at the fracture site, amplitude of micromotions and bigger global
335 movements compared to stainless steel nails. This tendency is related with the stiffness
336 of both materials: steel nails provide stiffer osteosyntheses than the titanium nails.

337

338 The obtained results agree with previous experiences using anterograde intramedullary
339 nails. So, anterograde interlocked intramedullary nails have been used successfully in a
340 wide range of fracture types: in the treatment of extra articular distal femoral fractures
341 with 7 cm of intact distal femur, or when a 7 cm fragment could be reconstructed with
342 accessory lag screws or distal locking screws [44].

343

344 However, contraindications to anterograde nailing are a pre-existing proximal prosthesis
345 or hardware, femoral deformity, obliteration of the intramedullary canal, and
346 insufficient distal bone stock [43, 45].

347

348 **5.-CONCLUSIONS**

349

350 The FE models developed allow the simulation of fracture in different locations, with
351 different gap and different alternatives of nailing, in accordance with the clinical cases
352 included in the follow-up, and determine whether the relative displacement at fracture
353 site fall within acceptable limits, in order to achieve the fracture healing.

354

355 There is a good agreement between clinical results and the simulated fractures in terms
356 of gap size. Non-comminuted fractures have the minimum mean consolidation time,
357 which coincides with the appropriate mobility at fracture site obtained in the FE
358 simulations, whereas comminuted fractures have the higher mean consolidation period,
359 corresponding to the excessive mobility at fracture site obtained by means of FE
360 simulations. The healing time increases inasmuch as the comminution grade is higher.

361

362 In view of the correspondence between clinical follow-up and simulation results, it is
363 clear that the biomechanical behaviour of the different osteosyntheses, without forget
364 other biological and physiological factors, determines the appropriate fracture healing.

365

366 Considering the obtained results, it can be asserted that the anterograde locked nail is
367 particularly useful in the treatment of a wide range of supracondylar fractures with
368 proximal extension into the femoral diaphysis.

369

370 **List of abbreviations used**

371 IM: Intramedullary Nailing

372 FE: Finite Element

373 3D: Three-Dimensional

374 CT: Computed Tomography

375 CAD: Computed Aided Design

376 PO: Pos-operative

377

378 **Authors' contributions**

379 AH, JA and LG conceived the design of study. LG, SG, EI and SP conceived and
380 developed the finite element models and carried out all the simulations. AH and JA
381 realized the medical supervision of models. All authors participated in the drawing up
382 of the manuscript, and read and approved the final manuscript.

383

384 **Acknowledgements**

385 This research has been partially financed by The Fundacion Mutua Madrileña (Research
386 Projects: AP162632016) and by the Government of Spain: Ministry of Economy and
387 Competitiveness (Research Project: DPI2016-77745-R).

388

389 **Competing interests**

390 None declared

391

392 **References**

- 393 1. Braten M, Terjesen T, and Rossvoll I, Femoral shaft fractures treated by intramedullary
394 nailing. A follow-up study focusing on problems related to the method. *Injury* 1995;**26**:
395 379-83.
- 396 2. Wolinsky P, Tejwani N, Richmond JH, Koval KJ, Egol K, and Stephen DJ,
397 Controversies in intramedullary nailing of femoral shaft fractures. *Instr Course Lect*
398 2002;**51**: 291-303.
- 399 3. G. K, Die Marknalung von Knochenbruchen. Langenbecks. *Arch Klin Chir* 1940;**200**:
400 443-55.
- 401 4. Wiss DA, Fleming CH, Matta JM, and Clark D, Comminuted and rotationally unstable
402 fractures of the femur treated with an interlocking nail. *Clin Orthop Relat Res* 1986:
403 35-47.
- 404 5. Winqvist RA, Locked Femoral Nailing. *J Am Acad Orthop Surg* 1993;**1**: 95-105.
- 405 6. Sha M, et al., The effects of nail rigidity on fracture healing in rats with osteoporosis.
406 *Acta Orthop* 2009;**80**: 135-8.
- 407 7. Epari DR, Kassi JP, Schell H, and Duda GN, Timely fracture-healing requires
408 optimization of axial fixation stability. *J Bone Joint Surg Am* 2007;**89**: 1575-85.
- 409 8. Kenwright J and Goodship AE, Controlled mechanical stimulation in the treatment of
410 tibial fractures. *Clin Orthop Relat Res* 1989: 36-47.
- 411 9. Ehlinger M, Ducrot G, Adam P, and Bonnomet F, Distal femur fractures. Surgical
412 techniques and a review of the literature. *Orthop Traumatol Surg Res* 2013;**99**: 353-
413 60.
- 414 10. Court-Brown CM and Caesar B, Epidemiology of adult fractures: A review. *Injury*
415 2006;**37**: 691-7.
- 416 11. Gwathmey FW, Jr., Jones-Quaidoo SM, Kahler D, Hurwitz S, and Cui Q, Distal
417 femoral fractures: current concepts. *J Am Acad Orthop Surg* 2010;**18**: 597-607.

- 418 12. Shih KS, Hsu CC, and Hsu TP, A biomechanical investigation of the effects of static
419 fixation and dynamization after interlocking femoral nailing: a finite element study. *J*
420 *Trauma Acute Care Surg* 2012;**72**: E46-53.
- 421 13. Tupis TM, Altman GT, Altman DT, Cook HA, and Miller MC, Femoral bone strains
422 during antegrade nailing: a comparison of two entry points with identical nails using
423 finite element analysis. *Clinical biomechanics (Bristol, Avon)* 2012;**27**: 354-9.
- 424 14. Ricci WM, Gallagher B, and Haidukewych GJ, Intramedullary nailing of femoral shaft
425 fractures: current concepts. *J Am Acad Orthop Surg* 2009;**17**: 296-305.
- 426 15. Kaiser MM, et al., Biomechanical analysis of a synthetic femoral spiral fracture model:
427 Do end caps improve retrograde flexible intramedullary nail fixation? *Journal of*
428 *Orthopaedic Surgery and Research* 2011;**6**.
- 429 16. Wang CJ, Brown CJ, Yettram AL, and Procter P, Intramedullary femoral nails: one or
430 two lag screws? A preliminary study. *Medical engineering & physics* 2000;**22**: 613-24.
- 431 17. Wang CJ, Brown CJ, Yettram AL, and Procter P, Intramedullary nails: some design
432 features of the distal end. *Medical engineering & physics* 2003;**25**: 789-94.
- 433 18. Sitthiseripratip K, et al., Finite element study of trochanteric gamma nail for
434 trochanteric fracture. *Med Eng Phys* 2003;**25**: 99-106.
- 435 19. Cheung G, Zalzal P, Bhandari M, Spelt JK, and Papini M, Finite element analysis of a
436 femoral retrograde intramedullary nail subject to gait loading. *Med Eng Phys* 2004;**26**:
437 93-108.
- 438 20. Filardi V and Montanini R, Measurement of local strains induced into the femur by
439 trochanteric Gamma nail implants with one or two distal screws. *Med Eng Phys*
440 2007;**29**: 38-47.
- 441 21. Chen SH, Yu TC, Chang CH, and Lu YC, Biomechanical analysis of retrograde
442 intramedullary nail fixation in distal femoral fractures. *Knee* 2008;**15**: 384-9.
- 443 22. Perez A, Mahar A, Negus C, Newton P, and Impelluso T, A computational evaluation
444 of the effect of intramedullary nail material properties on the stabilization of simulated
445 femoral shaft fractures. *Medical Engineering & Physics* 2008;**30**: 755-760.
- 446 23. Shih KS, Tseng CS, Lee CC, and Lin SC, Influence of muscular contractions on the
447 stress analysis of distal femoral interlocking nailing. *Clinical Biomechanics* 2008;**23**:
448 38-44.
- 449 24. Montanini R and Filardi V, In vitro biomechanical evaluation of antegrade femoral
450 nailing at early and late postoperative stages. *Medical Engineering & Physics* 2010;**32**:
451 889-897.
- 452 25. Salas C, Mercer D, DeCoster TA, and Reda Taha MM, Experimental and probabilistic
453 analysis of distal femoral periprosthetic fracture: a comparison of locking plate and
454 intramedullary nail fixation. Part A: experimental investigation. *Comput Methods*
455 *Biomech Biomed Engin* 2011;**14**: 157-64.
- 456 26. Salas C, Mercer D, DeCoster TA, and Reda Taha MM, Experimental and probabilistic
457 analysis of distal femoral periprosthetic fracture: a comparison of locking plate and
458 intramedullary nail fixation. Part B: probabilistic investigation. *Comput Methods*
459 *Biomech Biomed Engin* 2011;**14**: 175-82.
- 460 27. Shih KS, Hsu CC, and Hsu TP, A biomechanical investigation of the effects of static
461 fixation and dynamization after interlocking femoral nailing: A finite element study.
462 *Journal of Trauma and Acute Care Surgery* 2012;**72**: E46-E53.
- 463 28. Siemens, *I-deas® 11 NX Series PLM software*
464 [<http://www.plm.automation.siemens.com/>] 2013: Plano (Texas).
- 465 29. Gabarre S, Herrera A, Mateo J, Ibarz E, Lobo-Escolar A, and Gracia L, Study of the
466 polycarbonate-urethane/metal contact in different positions during gait cycle. *Biomed*
467 *Res Int* 2014;**2014**: 548968.
- 468 30. Herrera A, Panisello JJ, Ibarz E, Cegonino J, Puertolas JA, and Gracia L, Long-term
469 study of bone remodelling after femoral stem: A comparison between dxa and finite
470 element simulation. *Journal of Biomechanics* 2007;**40**: 3615-3625.

- 471 31. Claes LE, Wilke HJ, Augat P, Rubenacker S, and Margevicius KJ, Effect of
472 dynamization on gap healing of diaphyseal fractures under external fixation. *Clin*
473 *Biomech (Bristol, Avon)* 1995;**10**: 227-234.
- 474 32. Yamaji T, Ando K, Wolf S, Augat P, and Claes L, The effect of micromovement on
475 callus formation. *J Orthop Sci* 2001;**6**: 571-5.
- 476 33. Augat P, Burger J, Schorlemmer S, Henke T, Peraus M, and Claes L, Shear movement
477 at the fracture site delays healing in a diaphyseal fracture model. *J Orthop Res* 2003;**21**:
478 1011-7.
- 479 34. Chen SH, Chiang MC, Hung CH, Lin SC, and Chang HW, Finite element comparison
480 of retrograde intramedullary nailing and locking plate fixation with/without an
481 intramedullary allograft for distal femur fracture following total knee arthroplasty. *Knee*
482 2014;**21**: 224-31.
- 483 35. Grant JA, Bishop NE, Gotzen N, Sprecher C, Honl M, and Morlock MM, Artificial
484 composite bone as a model of human trabecular bone: the implant-bone interface. *J*
485 *Biomech* 2007;**40**: 1158-64.
- 486 36. Eberle S, Gerber C, von Oldenburg G, Hungerer S, and Augat P, Type of Hip Fracture
487 Determines Load Share in Intramedullary Osteosynthesis. *Clinical Orthopaedics and*
488 *Related Research* 2009;**467**: 1972-1980.
- 489 37. Samiezadeh S, Tavakkoli Avval P, Fawaz Z, and Bougherara H, Biomechanical
490 assessment of composite versus metallic intramedullary nailing system in femoral shaft
491 fractures: A finite element study. *Clin Biomech* 2014;**29**: 803-10.
- 492 38. Villavicencio AT, Burneikiene S, Bulsara KR, and Thramann JJ, Perioperative
493 complications in transforaminal lumbar interbody fusion versus anterior-posterior
494 reconstruction for lumbar disc degeneration and instability. *J Spinal Disord Tech*
495 2006;**19**: 92-7.
- 496 39. Winquist RA and Hansen ST, Jr., Comminuted fractures of the femoral shaft treated by
497 intramedullary nailing. *Orthop Clin North Am* 1980;**11**: 633-48.
- 498 40. Kwong FN and Harris MB, Recent developments in the biology of fracture repair. *J Am*
499 *Acad Orthop Surg* 2008;**16**: 619-25.
- 500 41. Claes L, Eckert-Hubner K, and Augat P, The effect of mechanical stability on local
501 vascularization and tissue differentiation in callus healing. *J Orthop Res* 2002;**20**:
502 1099-105.
- 503 42. Simon U, Augat P, Utz M, and Claes L, A numerical model of the fracture healing
504 process that describes tissue development and revascularisation. *Computer Methods in*
505 *Biomechanics and Biomedical Engineering* 2011;**14**: 79-93.
- 506 43. Albert MJ, Supracondylar Fractures of the Femur. *J Am Acad Orthop Surg* 1997;**5**:
507 163-171.
- 508 44. Leung KS, Shen WY, So WS, Mui LT, and Grosse A, Interlocking intramedullary
509 nailing for supracondylar and intercondylar fractures of the distal part of the femur. *J*
510 *Bone Joint Surg Am* 1991;**73**: 332-40.
- 511 45. Taylor JC, Treatment of Distal Femoral Fractures with the Russell-Taylor Nail.
512 *Techniques in Orthopaedics* 1994;**9**: 225-233.

513

514

515 **Figure legends**

516

517 **Figure 1.** Different kind of fractures with different gap sizes: 0.5 mm, 3 mm and 20

518 mm.

519 **Figure 2.** Interaction between nail and bone and between screws and nail

520 **Figure 3.** Boundary conditions

521 **Figure 4.** Deformed shape (x25) and vertical displacement maps corresponding to distal

522 fractures: a) non-comminuted (gap size 0.5 mm); b) comminuted (gap size 20 mm).

523 **Figure 5.** Homologue points for micromotion processing: anterior and posterior view.

524 **Figure 6.** Comparative mechanical behaviour scheme between proximal and distal

525 fractures (deformed shape x50)


526

527 **Tables**

528

529 **Table 1.** *List of FE models according screw combination*

Model	Proximal screws	Distal screws	Fracture location	Gap size
1			Proximal	0.5 mm.
2	Oblique (#1)	2 L/M screws (#2,3)	Medial	3.0 mm. 20 mm.
3			Distal	



530

531 **Table 2.** *Statistics for the clinical follow-up*

Wiss zone	Cases	Conminution grade	Cases
2	7	None	29
3	11	1	9
4	22	2	9
5	15	3	1
		4	7
Total	55		55

532

533

534

535

536

537 **Table 3a.** Gap strain verification according to Perren [μm]. Nail made of 316 LVM.

PERREN METHOD			
# Model	% ϵ 0.5 mm.	% ϵ 3.0 mm.	% ϵ 20.0 mm.
Proximal	12.06	2.20	0.45
Medial	10.39	1.79	0.37
Distal	8.14	1.61	0.33

538

539 **Table 3b.** Gap strain verification according to Perren [μm]. Nail made of Ti-6Al-4V.

PERREN METHOD			
# Model	% ϵ 0.5 mm.	% ϵ 3.0 mm.	% ϵ 20.0 mm.
Proximal	18.61	3.34	0.70
Medial	15.18	3.59	0.70
Distal	12.40	3.06	0.62

540

541 **Table 4a.** Amplitude of axial micromotion [μm]. Nail made of 316 LVM.

Maximum amplitude of micromotion [μm]			
# Model	GAP 0.5 mm	GAP 3 mm	GAP 20 mm
Proximal	60.29	66.13	90.29
Medial	51.96	53.77	73.39
Distal	40.69	48.33	66.43

542

543 **Table 4b.** Amplitude of axial micromotion [μm]. Nail made of Ti-6Al-4V.

Maximum amplitude of micromotion [μm]			
# Model	GAP 0.5 mm.	GAP 3 mm.	GAP 20 mm.
Proximal	93.07	100.13	140.83
Medial	75.88	107.81	139.80
Distal	62.02	91.87	123.71

544

545

546

547

548

549

550

Table 5a. Global movement at the top of the nail [mm]. Nail made of 316 LVM.

Global movement of the top of nail [mm]			
# Model	GAP 0.5 mm.	GAP 3 mm.	GAP 20 mm.
Proximal	1.33	1.35	1.38
Medial	1.53	1.54	1.67
Distal	1.75	1.85	2.01

551

552

Table 5b. Global movement at the top of the nail [mm]. Nail made of Ti-6Al-4V.

Global movement of the top of nail [mm]			
# Model	GAP 0.5 mm.	GAP 3 mm.	GAP 20 mm.
Proximal	1.62	1.65	1.73
Medial	1.98	2.01	2.26
Distal	2.36	2.85	3.14

553

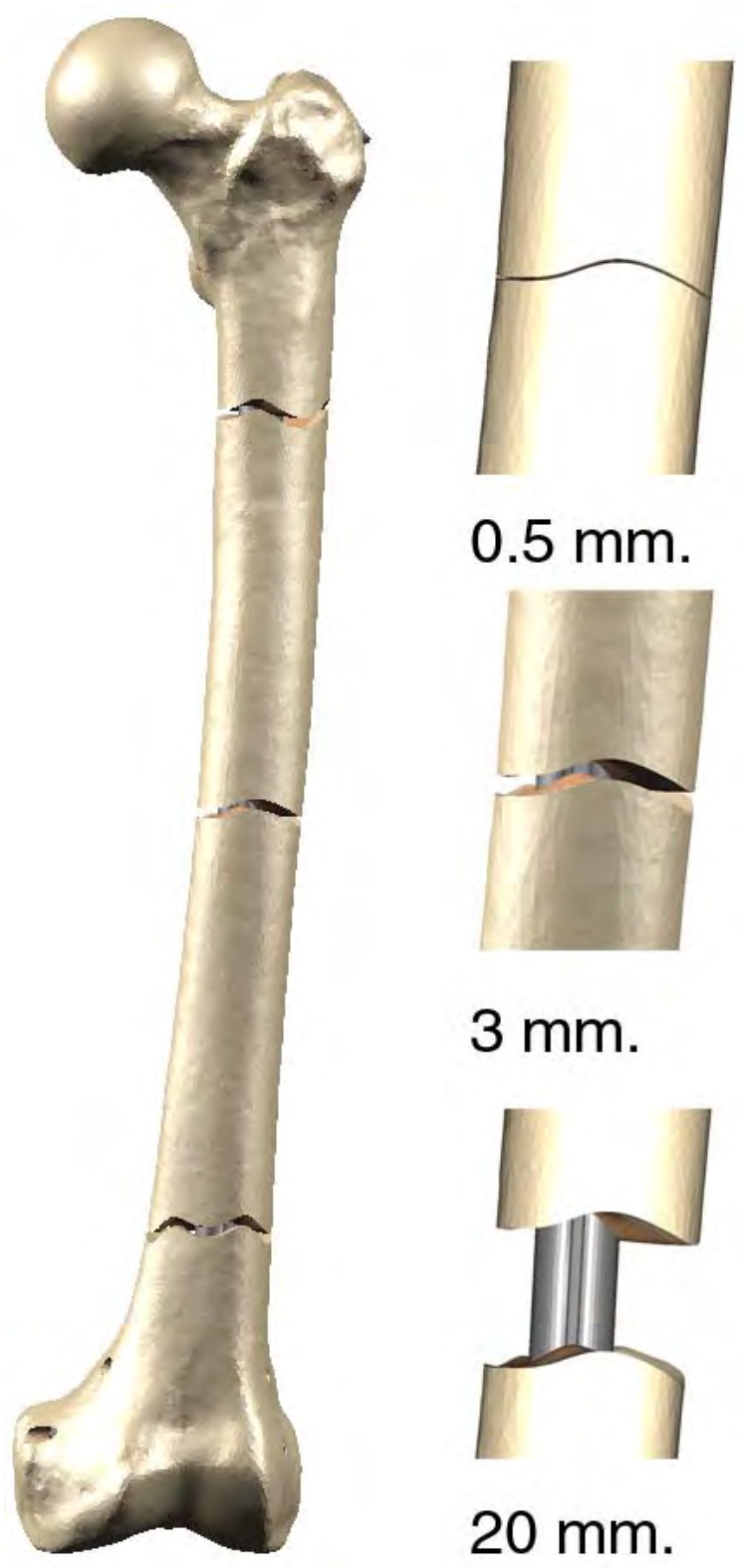
554

555

556

557 **Figures**

558



559

560 **Figure 1.** Different kind of fractures with different gap sizes: 0.5 mm, 3 mm and 20 mm.



561

562

Figure 2. Interaction between nail and bone and between screws and nail

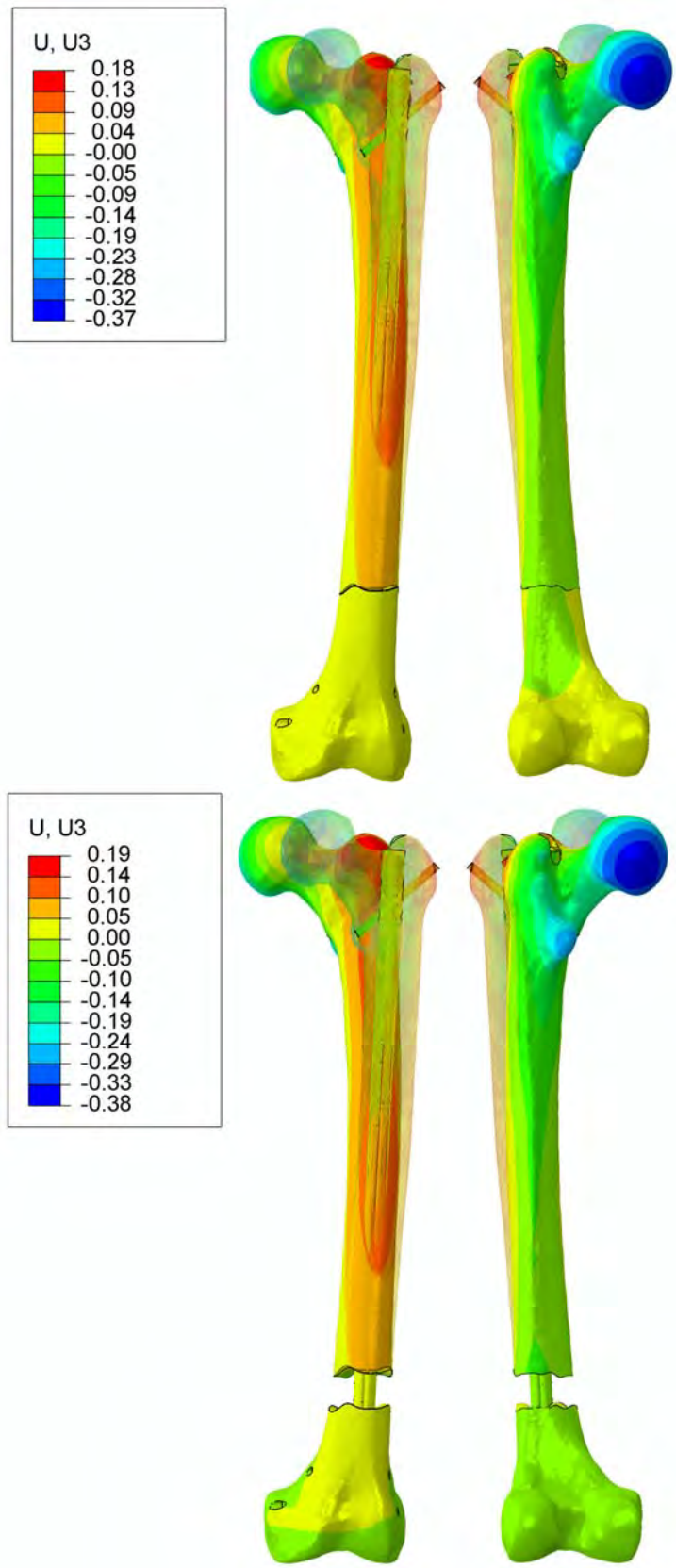


563

564

Figure 3. Boundary conditions

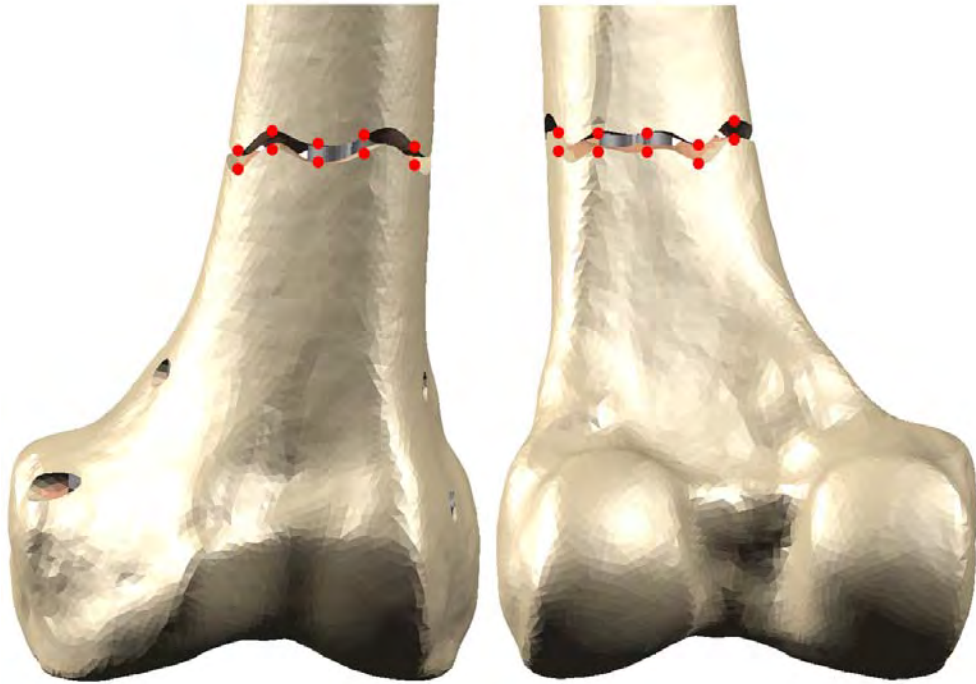
565



566

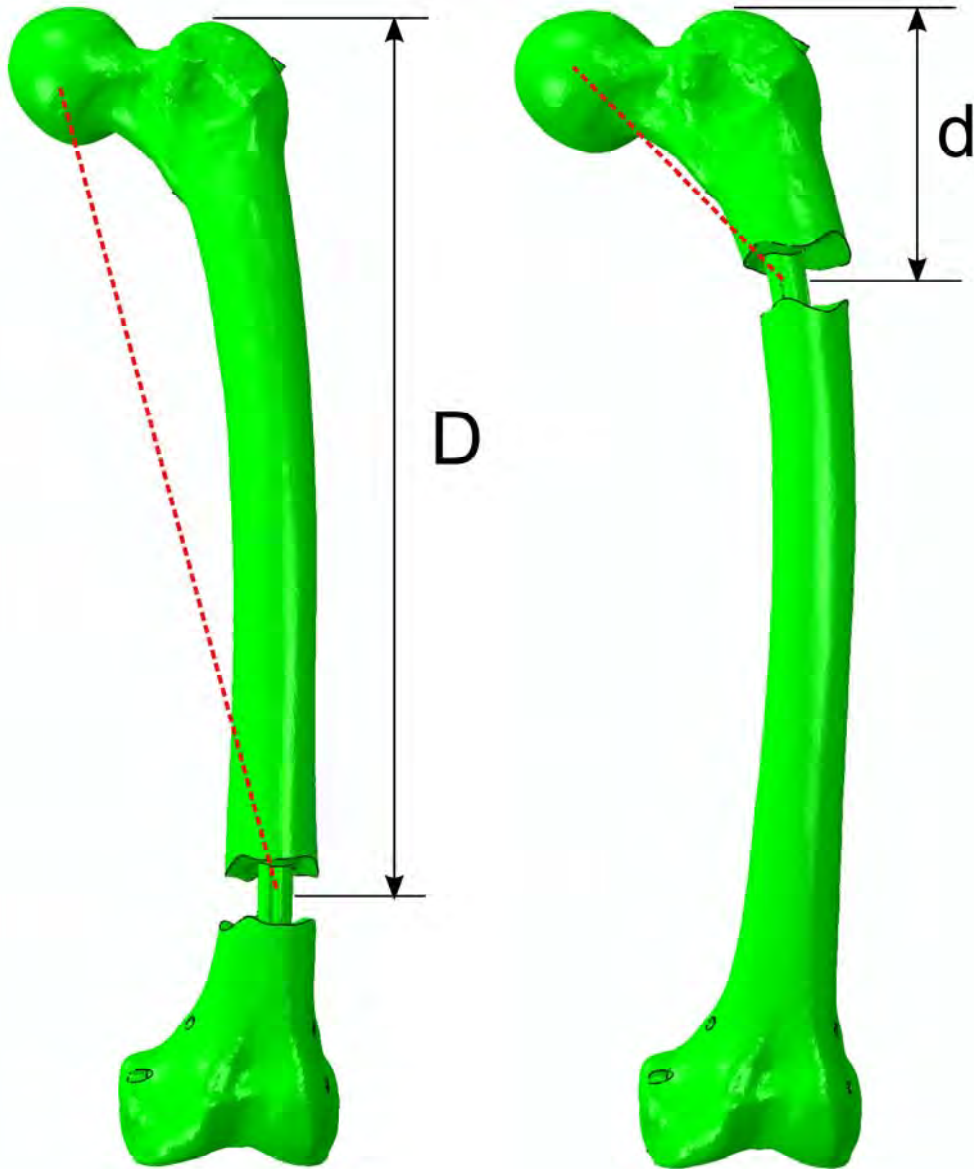
567

568 **Figure 4.** Deformed shape (x25) and vertical displacement maps corresponding to distal
 569 fractures: a) non-comminuted (gap size 0.5 mm); b) comminuted (gap size 20 mm)



570
571
572

Figure 5. Homologue points for micromotion processing: anterior and posterior view.



573

574 **Figure 6.** Comparative mechanical behaviour scheme between proximal and distal fractures
575 (deformed shape x50)

576